Photodegradation of Atmospheric Chromophores: Changes in Oxidation State and Photochemical Reactivity

Zhen Mu[a], Qingcai Chen[a*], Lixin Zhang[a], Dongjie Guan[a] and Hao Li[a]

[a] *School of Environmental Science and Engineering, Shaanxi University of Science and Technology, Xi'an 710021, China*

*Corresponding authors:

School of Environmental Science and Engineering, Shaanxi University of Science and

Technology, Weiyang District, Xi'an, Shaanxi, 710021, China.

*(Q. C.) Phone: (+86) 0029-86132765; e-mail: chenqingcai@sust.edu.cn;

Abstract: Atmospheric chromophoric organic matter (COM) can participate in photochemical reactions because of the photosensitiveness, thus COM have a potential contribution to aerosols aging. The photochemical mechanism of atmospheric COM and the effect of photo-degradation on its photochemical reactivity are not fully understood. Here, we report the characteristics of COM photo-degradation, the potential effects of COM photolysis on the photochemical reactivity, and the contribution of COM to reactive oxygen species (ROS). COM are identified by excitation-emission matrices combined with parallel factor analysis. We confirm that both water-soluble and water-insoluble COM are photo-bleached, and an average 70% of fluorescence intensities are lost after 7 days of light exposure. Furthermore, there is a transformation from low oxidation to high oxidation HULIS and high oxidation HULIS could be used to trace the degree of aerosols aging. In terms of photochemical reactivity, compared with before photolysis, the triplet state COM ($^3COM^*$) decrease slightly in ambient particulate matter (ambient PM) samples, but increase in primary organic aerosol (POA). The result also highlight that the photochemical mechanisms and aerosol aging processes are relatively different in various aerosols. Photolysis and conversion of COM reduce photochemical activity, so that COM induce less singlet oxygen. In conclusion, photo-degradation of COM not only change the chemical compositions, but also change the roles of the COM in aerosol aging.

Key word: atmospheric chromophores; photo-degradation; EEMs; triplet state; reactive oxygen species.

TOC:
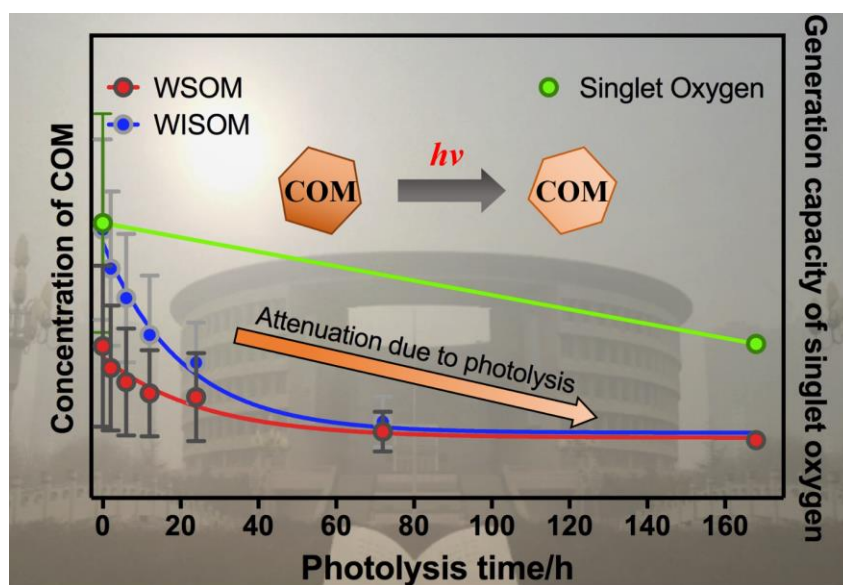
1. Introduction

Chromophoric organic matter (COM) widely exists in the atmospheric environment. COM are mainly derived from biomass combustion emissions and secondary chemistry reactions (Andreae and Gelencser, 2006; Graber and Rudich, 2005; Zappoli et al., 1999). Because of the significant absorption for short wave radiation (the range of near-ultraviolet light to visible light) (Rosario-Ortiz and Canonica, 2016; Cheng et al., 2016), COM may photolyze, convert components and induce reactive substances (Chen et al., 2018; Wenk et al., 2011; Maizel et al., 2017). Therefore, simulation and evaluation of COM photochemistry is necessary for understanding aerosol aging.

As photosensitive substances in aerosol, the physical and chemical characteristics of COM change significantly under sunlight exposure (Kieber et al., 2012; Lee et al., 2013; McKnight et al., 2001; Murphy et al., 2013; Cory and McKnight, 2005; Korak et al., 2014; Chin et al., 1994). The specific impacts are summarized. (1) Changes in optical characteristics. Sunlight exposure cause the photo-bleaching of COM. Previous studies reported that chromophores produced by wood-burning were significantly photo-bleached in aerosols (Lee et al., 2014; Zhong and Jang, 2014). Murphy et al. reported that fluorescence intensity of chromophores decreased after 20 h of simulated solar irradiation (Murphy et al., 2018). Yet the mechanisms of photo-bleaching process are still not complete clear. (2) Changes in chemical composition. Photochemistry has a significant effect on the composition of COM. Photolysis can cause that COM decompose into small molecules and COM may have lower volatility and higher oxidation degree after photolysis (Vodacek et al., 1997; Del Vecchio and Blough, 2002; Gonsior et al., 2009; Grieshop et al., 2009). In contrast, COM could also be generated due to photochemical reaction. For example, oligomeric COM could be generated by a mixture of anthracene and naphthalene suspensions through self-oxidation under light conditions; photo-oxidation of aromatic isoprene oxides are an important source of high-molecular-weight COM (Altieri et al., 2006; Altieri et al., 2008; Haynes et al., 2019; Holmes and Petrucci, 2006; Perri et al., 2009). COM could also be generated after light exposure (Harrison et al., 2020). Changes in chemical composition affect photochemical activity in turn. Therefore, it is crucial to illustrate the changes in optical characteristics and chemical composition, which could promote understanding the characteristic and mechanisms of COM photochemistry in aerosols.

Atmospheric COM not only decompose and transform, but also participate in the complex photochemical reaction, which further affect the aerosol aging (Malley et al., 2017). On the one hand, COM could participate in atmospheric photochemical processes directly. For example, excited COM react with organic matter and generate secondary organic aerosols (Zhao et al., 2015; Saleh et al., 2013; Zhong and Jang, 2014; Lee et al., 2014; Liu et al., 2016). Various secondary photochemistry also increase the complexity of COM composition (Wenk et al., 2011; Zhou et al., 2019; Smith et al., 2014; Richards-Henderson et al., 2015; Kaur and Anastasio, 2018; Chen et al., 2016a and b). On the other hand, COM also participate in atmospheric photochemical reactions indirectly through inducing reactive species. Aromatic ketones could be excited to generate triplet state ($^3COM^*$) under light conditions (Rosario-Ortiz and Canonica, 2016; Del Vecchio and Blough,

61   2004; Wenk et al., 2013; Ma et al., 2010). $^3COM^*$ induce reactive oxygen species (ROS), such as

62   singlet oxygen ($^1O_2$), super-oxygen ($\cdot O_2^-$) and hydroxyl ($\cdot OH$), which could drive aerosol aging

63   (Paul Hansard et al., 2010; Szymczak and Waite, 1988; Zhang et al., 2014; Rosario-Ortiz and

64   Canonica, 2016; Sharpless, 2012; Haag and Gassman, 1984). Photochemical activity is also

65   universal feature of dissolved organic carbon (DOC). Powers et al. (2015) probed the photochemical

66   activity of the deep ocean refractory DOC through simultaneous measuring the rates of both H_2O_2

67   and O_2^- photoproduction in laboratory. It is necessary to clarify the path and effect of COM driving

68   aerosol aging, but the path and effect are both unclear.

69   The chemical composition and atmospheric quality are significantly affected by aerosol aging.

70   In order to illustrate the properties of COM and the effect of COM photolysis on aerosol aging, we

71   simulate the process of COM photolysis and COM inducing ROS in primary organic aerosol (POA)

72   and ambient particulate matter (ambient PM) in laboratory. The characteristics of photo-degradation

73   in water-soluble and water-insoluble chromophores are clarified by the approach of excitation-

74   emission matrices (EEM) combined with parallel factor analysis (PARAFAC). The effects of COM

75   on photochemical reactivity and aerosol aging (photochemical reactivity is characterized by triplet

76   state and singlet oxygen generation capacity) are also stated by the method of reactive species

77   capture technology and electron paramagnetic resonance spectrometer (EPR).

78   2. Experimental Section

79   *2.1 Sample Collection*

80   A total of 16 samples were collected (The details of the samples are shown in Table S1 of SI).

81   The ambient PM samples were collected in Shaanxi University of Science and Technology, Xi'an,

82   Shaanxi Province (N34°22′35.07″, E108°58′34.58″; the sampling device is about 30 m from the

83   ground). The ambient PM samples were collected on quartz fiber filter (Pall life sciences, Pall

84   Corporation, America) by an intelligent large-flow sampler (Xintuo XT-1025, Shanghai, China)

85   with a sampling time of 23 h 30 min and a sampling flow rate of 1000 L/min. The ambient PM

86   samples were stored in the refrigerator at -20 ℃ prior to use.

87   The POA samples were collected through a combustion chamber. Straw and coal burning are

88   the main way of heating and cooking in the rural areas in China. Therefore, the combustion of wheat

89   straw, corn straw, rice straw and wood were chosen to generate aerosols. As shown in **Fig.1**, Wheat

90   straw, corn straw, rice straw and wood were burned in the annular combustion chamber when

91   temperatures rose to 500 ℃. The clean air was introduced at a flow rate of 2 L/min to ensure

92   complete combustion. The particle matter entered the mixing box. The clean air was introduced into

93   mixing box at a flow rate of 2 m^3/h to dilute the combustion gas. POA samples were collected on

94   the quartz filter (Pall life sciences, Pall Corporation, America) with a diameter of 37 mm. The POA

95   sample were stored in the refrigerator at -20 ℃ prior to use.

96
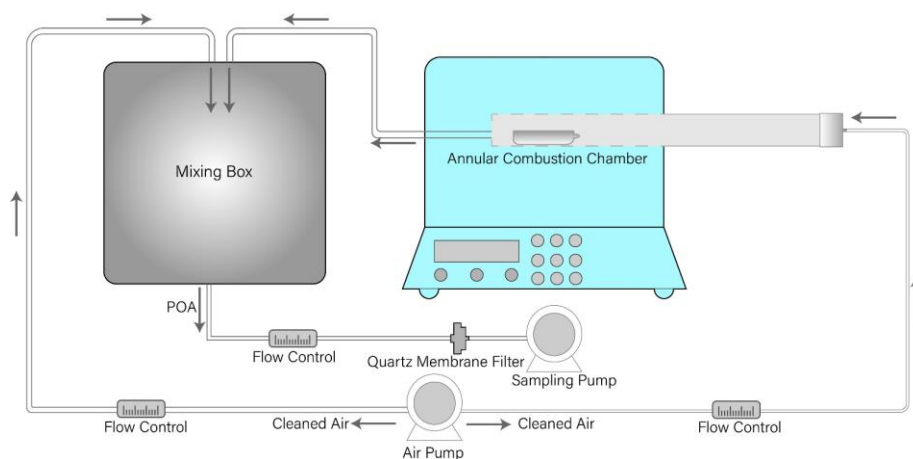
97 **Fig.1** Schematic diagrams of combustion equipment for POA.

98 *2.2 Photolysis experiment*

99   The material of reactor is quartz (**Fig.2a**) and the reactor was designed for photolysis

100 experiment. The reactor was sealed through clamping a quartz cover to reactor. Two air vents was

101 used to air exchange and Two water cycle vents were connected to water circulator to ensure that

102 the temperature was about 25°C in the reactor. The reactor was placed on a magnetic stirrer and the

103 rotation speed was 200 rmp to stabilize the temperature and humidity (~50%). A xenon lamp was

104 equipped with a VISREF light filter (PLS-SXE 300, Perfectlight, China) to simulate sunlight (The

105 wavelength spectrum of the xenon lamp is shown in Figure S1 of SI). The light intensity per unit

106 area was about 1.2-1.3 times the solar light at 12:00, at N34°22′35.07″, E108°58′34.58″. A small

107 storage platform was placed in the reactor to place quartz reaction cell (**Fig.2b**) and quartz plate

108 (**Fig.2c**). The illumination times were 0 h, 2 h, 6 h, 12 h, 24 h, 3 d and 7 d, respectively.

109

110

111
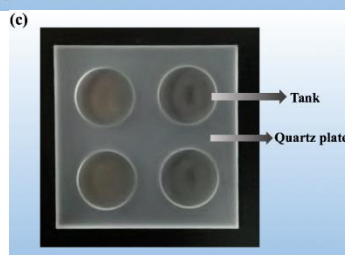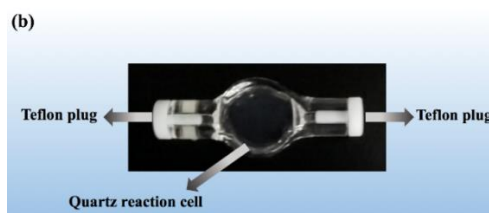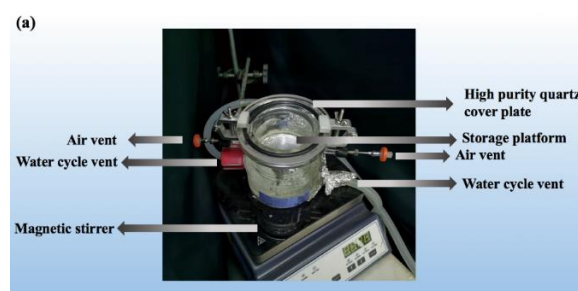
112 **Fig.2** Schematic diagrams of the photochemical devices. (a) The reactor is used for maintaining the reaction

113 environment. (b) The reactor is used for triplet state experiments. The reactor is made of quartz. The plugs are made

114 of Teflon. The internal volume is 200 µL. (c) A reactor is used for the experiment of triplet state inducing singlet

115 oxygen. The size of quartz plate is 35×35 mm^2. The size of the tanks is a radius of 5.6 mm and a depth of 2.5 mm.

116 *2.3 Sample extraction*

117 The samples extracts were obtained by the approach of ultrasonic extraction. The original and

118 photolyzed samples were extracted with ultra-pure water (>18.2 MΩ•cm, Master series, Hitech,

119 China) and the suspensions were filtered through a 0.45 µm filter (Jinteng, China) to obtain the

120 water-soluble organic matter (WSOM). After water extraction, the samples were further extracted

121 with methanol (HPLC Grade, Fisher Chemical, America) to obtain water-insoluble organic matter

122 (WISOM) using the above method. The blank samples were also extracted. The blank extraction

123 method was the same as sample extraction, which was used to correct the effect of the background.

124 *2.4 OC/EC analysis*

125 The method of organic carbon (OC) analysis could refer to the previous literature (Mu et al.,

126 2019). Briefly, 100 µL of extracts were injected on the clean quartz filter. Then, the filters were

127 dried out by a rotary evaporator. Carbonaceous components were analyzed by the OC/EC online

128 analyzer (Model 4, Sunset, America) with the approach of NIOSH 870 protocol (Karanasiou et al.,

129 2015). Six parallel samples were analyzed and the uncertainty of the method was <3.7% (one

130 standard deviation).

131 *2.5 Optical analysis*

132 The light absorption and EEM spectra of the extracts were measured by an Aqualog

133 fluorescence spectrophotometer (Horiba Scientific, America). The extracts were diluted for optical

134 analysis (The concentrations and dilution factors are shown in Table S2 of SI). The absorption

135 spectra were recorded in the wavelength range of 200-600 nm. The range of excitation wavelength

136 was 200-600 nm and the range of emission wavelength was 250-800 nm. The interval was 5 nm.

137 The exposure time was 0.5 s. Water and methanol background samples were measured using the

138 same method and the background signals were subtracted from the sample signals.

139 The EEM data was analyzed by the PARAFAC model to identify fluorophores (The detailed

140 analysis process refers to the previous papers) (Chen et al., 2016b; Chen et al., 2016a). 111 samples

141 were used to create the model. WSOM and WISOM were combined in the dataset to create the

142 PARAFC model. Briefly, according to the EEM characteristics and the residual error variation trend

143 of the 2-7 component PARAFAC models, 4 component PARAFAC model was selected (Analysis

144 error of the models are shown in Figure S2 of SI).

145 *2.6 Triplet state generation experiment*

146 The triplet states generation ability before and after photolysis were studied. Chemical probe

147 2,4,6-trimethylphenol (TMP) was used as the capturing agent for the triplet state. 60 µL of WSOM

148 extracts (OC concentrations are shown in Table S3) and 60 µL of TMP solution (c_{TMP} = 20 µM,

149 Aladdin, China) were mixed in the cell (**Fig.2b**). The cell was placed in the reactor (**Fig.2a**) and the

reaction conditions were the same as shown in 2.2. The illumination times was 0, 5, 10, 15, 30, 45, 60 and 90 min, respectively. 90 µL mixed solution was taken out from the cell at different time points. Then 30 µL of phenol solution (c_{phenol} = 50 µM, Aladdin, China) were added into the mixed solution (Phenol solution was used as the internal standard substance for TMP quantification). TMP was quantified by liquid chromatography (LC).

The analyzed parameters of LC are as follows: C18 column (Xuanmei, China); mobile phase: acetonitrile/water = 1/1 (v/v); flow rate: 1 mL/min; UV detector: detection wavelength 210 nm. The retention time is 14.5 min. Kaur and Anastasio (2018) and Richards-Henderson et al. (2015) have reported that TMP consumption conform to first-order kinetics in the triplet state capture reaction. The first-order kinetic equation was used to fit exponential relationship among the TMP concentration (c_{TMP}/µM), the illumination time (t/min) and triplet state generation rate constants (k_{TMP}/min^{-1}):

$$c_{TMP} = a \cdot e^{-t \times k_{TMP}} \tag{1}$$

2.7 Triplet state driving singlet oxygen experiment

The effects of the COM photolysis on singlet oxygen were studied. 4-Hydroxy-2, 2, 6, 6-tetramethylpiperidine (TEMP, c_{TEMP}=240 mM, Aladdin, China) was used as the capturing agent of singlet oxygen and captured singlet oxygen was quantified by EPR spectrometer (MS5000, Freiberg, Germany). Sorbic acid (SA, C_{SA}=133.3 µM, Aladdin, China) was used as quenching agent for triplet state. The method was as follows: (1) 40 µL WSOM, 40 µL TEMP and 40 µL ultra-pure water were mixed in the tanks (**Fig.2c**). The mixed solution was placed in the reactor (**Fig.2a**). Then, 50 µL of the mixed solution was taken out by capillary for EPR analysis; (2) 40 µL of WSOM, 40 µL of TEMP and 40 µL of ultra-pure water were mixed. The mixed solution was placed in the reactor for 60 min without illumination. Then 50 µL of the mixed solution was taken out by capillary for EPR analysis; (3) 40 µL of WSOM, 40 µL of TEMP and 40 µL of ultra-pure water were mixed in the cell. The mixed solution was placed in the reactor for 60 min with illumination. 50 µL of the mixed solution was taken out by capillary for EPR analysis; (4) 40 µL of WSOM, 40 µL of TEMP and 40 µL of SA solution were mixed in the cell. The mixed solution was placed in the reactor for 60 min with illumination, then 50 µL of the mixed solution was taken out by capillary for EPR analysis.

3. Results and discussion

3.1 Effect of COM photo-degradation on carbonaceous components

Organic matter can be decomposed and transformed in aerosol due to illumination (Wong et al., 2015). **Fig.3** describe the variable characteristics of total organic carbon and carbonaceous components before and after COM photolysis. The results show that both water-soluble and water-insoluble organic matter undergo partial photolysis in POA samples (**Fig.3A**), with an average decrease of 22.1% and 3.5%, respectively. WISOC decompose obviously in ambient PM than in POA, with an average decrease of 26.3%, while the WSOC do not change significantly in ambient PM (**Fig.3B**).

187   Photolysis also results in the variation on carbonaceous components. In POA (**Fig.3A**), the
188 relative content of the OC1 (OC1 and OC2-4 are the different stage in the process of thermal-optical
189 analysis) decrease, which is the main loss of OC. The organic matter in the OC1 stage are
190 characterized by small molecular weight and highly volatile (Karanasiou et al., 2015). The result
191 shows that OC1 has a stronger ability of photo-decompose. On the other hand, the pyrolysis carbon
192 (OPC) in WISOM show an increasing trend (an average increase of 2.4 times). Generally, the
193 pyrolysis carbon is oxygen-containing substance. Thus, the increase of oxygen-containing organics
194 may be due to the aerosols aging. In contrast to POA, the carbonaceous components are relatively
195 stable in ambient PM (**Fig.3B**). The result reflects that ambient PM samples have been subjected to
196 sufficient atmospheric oxidation, so organic matter are not decomposed or oxidized again.
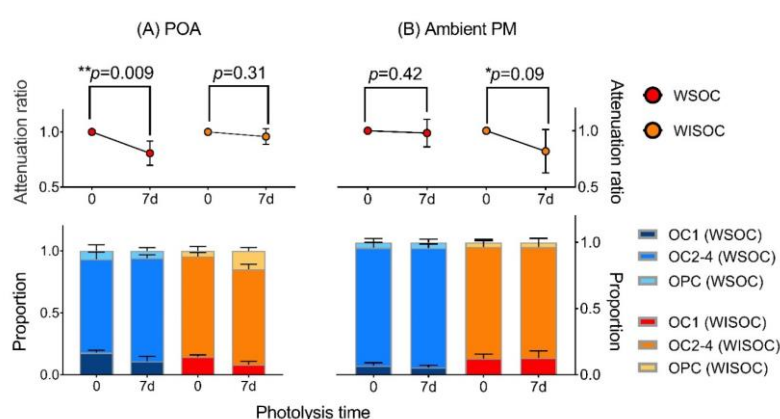
197
198 **Fig.3** Variations of total carbon and carbonaceous components before and after photolysis. The *p*-value is the
199 probability that two sets of data have the same level (two-tailed test). * and ** are represent the significant difference
200 at the 0.1 and 0.01 levels, respectively.

201 *3.2 Effect of COM photo-degradation on optical properties*

202   Both absorbance and total fluorescence volume (TFV, RU-nm2/m3) significantly decrease
203 during aerosol photolysis (Fig.4). Changes in optical properties are shown in Figure S3, S4 and S5.
204 The decrease of absorbance confirm that COM are photo-bleached (Duarte et al., 2005) and the
205 decay function of photolysis on absorbance is significant (Aiona et al., 2018). As shown in the
206 scatter plot (**Fig.4**), absorbance decreases significantly during photolysis. The decay kinetics of
207 absorbance is different to fluorophores. The attenuation trend is inconstant, so the decay kinetics do
208 not be mathematical analyzed and the absorbance also could confirm the photo-degradation of COM.
209 As shown in **Fig.4**, the attenuation of fluorescence is mathematical analyzed and the number or
210 shape of fluorophores do not change during COM photolysis. In POA (**Fig.4B**), TFV decrease by
211 74.8% on average and the attenuation characteristics of water-soluble and water-insoluble
212 components are similar. However, the attenuation of fluorescence intensities is different from
213 Aiona's paper (Aiona et al., 2018). The photolysis ability of COM is various and changes in

fluorescence intensities may depend on the types of COM and the photochemical environment. Exceptionally, the water-insoluble component of wood burning only decrease by 9.0% (Figure S5), which is significantly different from other POA samples. The attenuation of TFV and WISOC (section 3.1) are similar in wood burning samples, which probably attribute to the slight generation of secondary water-insoluble organic substances. The characteristics of TFV attenuation in ambient PM (rate constant $k = 0.04$ h^{-1}) is different from POA ($k = 0.07$ h^{-1}). Compared with water-soluble chromophores, the water-insoluble chromophores photo-decompose obviously and the TFV decrease by 79.1%, but water-soluble chromophores only 21.9% on average. The results suggest that COM have undergone a long-term atmospheric aging and water-soluble COM have greater ability to be photolyzed.
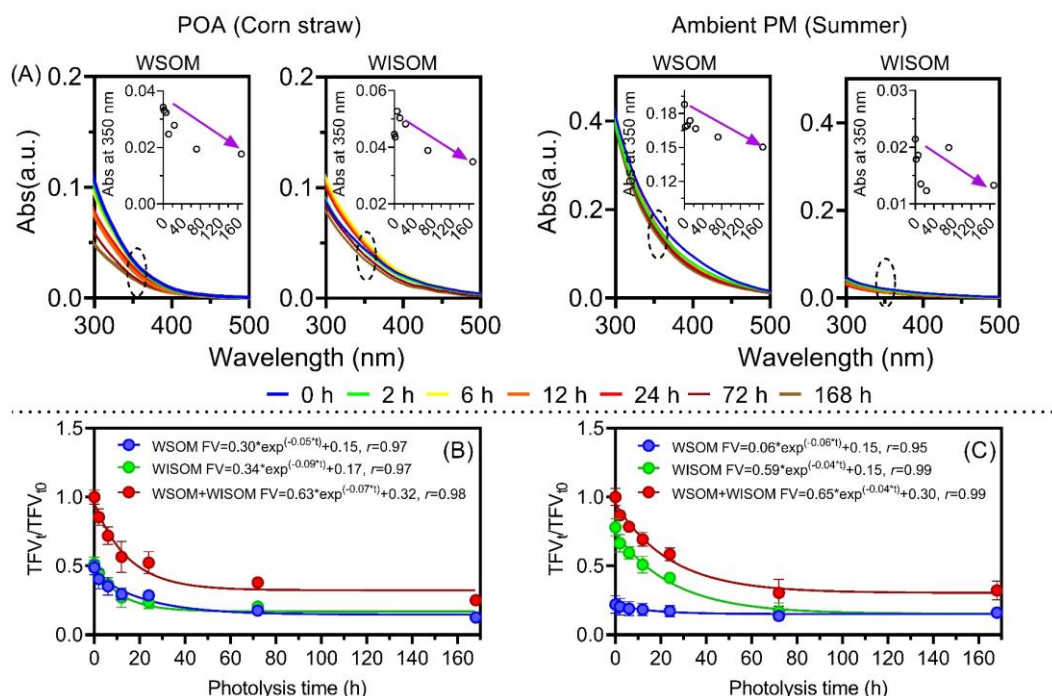
Fig.4 The changes of light absorption and fluorescence volume during the photolysis process. (A) The light absorption spectrum. The scatter plot is changes in Abs at 350 nm. (B) and (C) show the attenuation curve of average fluorescence volume of POA (except for the wood sample) and ambient PM samples, respectively.

Four types of COM are identified by the approach of EEMs-PARAFAC and the composition variations are studied (Fig.5A). Tang et al. (2020) study the chromophores in water-soluble and water-insoluble samples, respectively. However, based on the Chen's study (2020), water-soluble and water-insoluble samples were combined to create the PARAFAC model so that illustrate the distribution of chromophores in WSOM and WISOM. The fluorescence peaks of C1 and C2 appear at (Ex./Em. = 224/434 nm) and (Ex./Em. = 245/402 nm), and the peaks are similar to high and low oxidation HULIS, respectively (Chen et al., 2016b; Birdwell and Engel, 2010). The peaks of C3 and

C4 appear at (Ex./Em. = 220/354 nm) and (Ex./Em. = 277/329 nm) and these two fluorophores were associated with protein-like organic matter (PLOM-1 and PLOM-2) in previous studies (Sierra et al., 2005; Huguet et al., 2009; Chen et al., 2016a and 2016b; Coble, 2007; Fellman et al., 2009).

The compositions of chromophores change significantly during photolysis process. In POA (**Fig.5B**), the high-oxidation HULIS increase significantly in water-soluble component and the relative content increase by 25.7% on average. On the contrary, low oxidation HULIS and PLOM decrease by 6.0% and 19.7%, respectively. The proportion variation indicates that high-oxidation HULIS chromophores could be generated and low oxidation HULIS and PLOM chromophores may be photolyzed (Tang et al., 2020; Chen et al., 2020). Not only in water-soluble chromophores, the content of high-oxidation HULIS also increase in water-insoluble chromophores (average 17.5%) and low-oxidation HULIS also decrease in water-insoluble chromophores. In ambient PM, the content of high-oxidation HULIS increase and the low-oxidation HULIS decrease (**Fig.5C**), which reveal that low-oxidation HULIS could be transformed into high-oxidation HULIS (Chen et al., 2016a). Thus, high-oxidation HULIS could be used to trace the degree of aerosols aging.
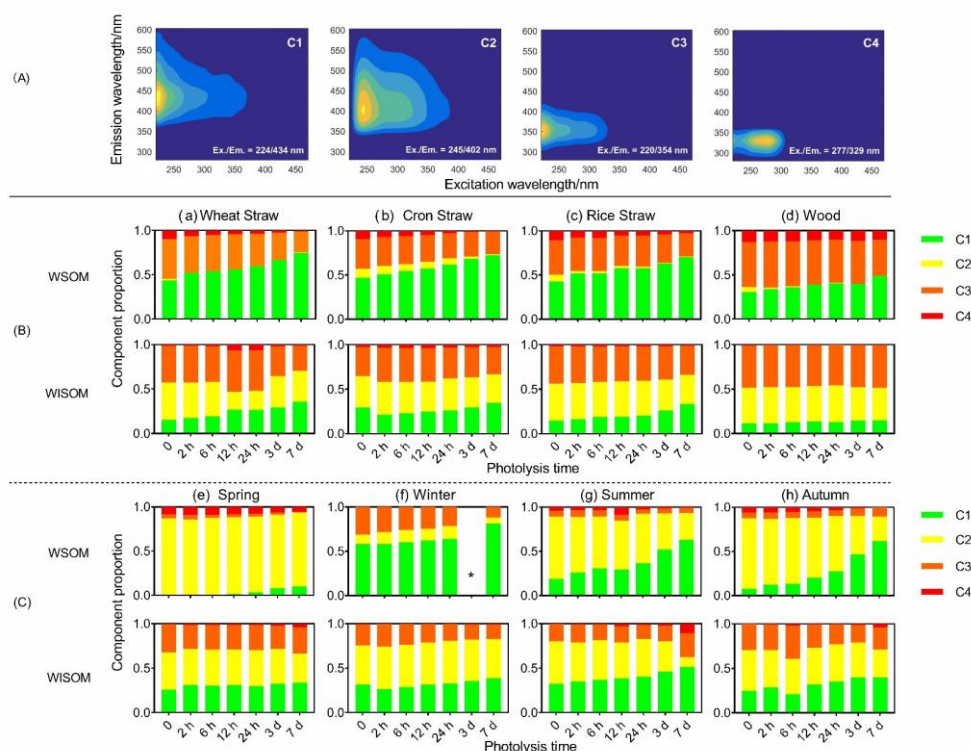
Fig.5 (A) The EEM spectra of chromophores; (B) is the variation characteristics of chromophores in POA; (C) is the variation characteristics of chromophores in ambient PM. *: The data of 3-day photolysis of water-soluble chromophores in winter is unavailable.

3.3 Effect of COM photo-degradation on aerosol photochemical reactivity

COM photo-degradation has a significant effect on aerosol photochemical reactivity. The photochemical activity is characterized by the generating ability of $^3COM^*$ and singlet oxygen. **Fig.6** show the difference of triplet state generation capability before and after the photolysis

257 (Details are shown in Figure S6 of SI). In ambient PM, the generation rate of triplet state is decreased
258 by 11% on average after COM photolysis, while statistical analysis shows that photo-degradation
259 does not significantly affect the triplet state generation ($p = 0.38$, two-tailed test). On the contrary,
260 the triplet states generation rate markedly increases by 75% on average in POA ($p = 0.07$, two-tailed
261 test), which indicate that photo-degradation significantly promote triplet state generation. COM are
262 photo-decomposed, while the triplet state generation ability remains unchanged or increase. The
263 results are not as expected. However, the result can be explained by recent study (Chen et al. 2020
264 for ACPD): only a small number of chromophores have the ability to generate triplet states in
265 aerosols. The decomposition of most chromophores do not represent the decomposition of these
266 specific types of chromophores. We use a high concentration of TMP, in this case, TMP mainly
267 capture short-lived triplet state (Rosado-Lausell et al., 2013). Thus, chromophores that can form a
268 short-lived triplet state may not be reduced or even generated during the photolysis process.
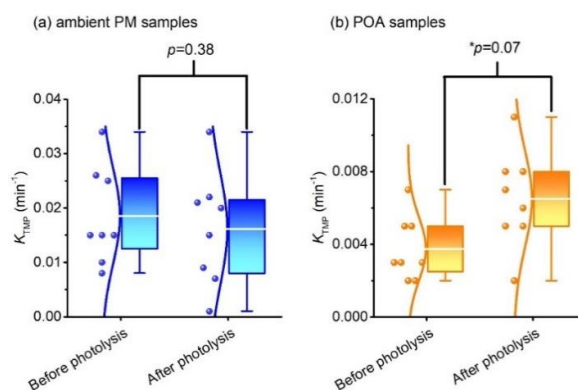
269
270 **Fig.6** The changes of the triplet state generation capacity in (a) ambient PM and (b) POA samples before and after
271 photolysis. The line from bottom to top in the box plots are minimum, first quartile, the average value (white lines),
272 third quartile, and maximum, respectively. The p-value is the probability that two sets of data have the same level
273 (two-tailed test). * represents a significant difference at the 0.1 level.

274   COM can generate triplet states and furtherly induce singlet oxygen (McNeill and Canonica,
275 2016). The effects of COM photo-degradation on singlet oxygen are illustrated using chemical
276 capture and EPR analysis. Typical EPR spectra of $^1O_2$ are shown in **Fig.7** (EPR spectra of all
277 samples are shown in Figure S7 and Figure S8). More narrowly, in the original POA samples (i.e.,
278 the sample with photolysis time is 0, details of samples are described in section 2.2), there is no
279 significant $^1O_2$ signal before light excitation (the red curve in **Fig.7A (I)**) and only a small amount
280 of $^1O_2$ is generated after 60 min in dark (the red curve in **Fig.7A (II)**), which indicated that POA
281 has certain oxidability. As expected, compared with the samples without light excitation (the red
282 curve in **Fig. 7A (I)**), the signal intensity of $^1O_2$ increases by a factor of 3 after 60 minutes of light
283 excitation (the red curve in **Fig. 7A (III)**), which prove the significant promoting effect of light on
284 $^1O_2$. However, $^1O_2$ is not reduced when the triplet state is quenched by sorbic acid (the red curve in
285 **Fig.7A (IV)**). Sorbic acid is a trapping agent of high-energy triplet state (triplet energies $E_T = 239$-

286 247 kJ/mol) (Zhou et al., 2019; Moor et al., 2019), therefore, the above results indicate that the low-

287 energy $^3COM^*$ (E_T <239 kJ/mol) may be the main precursor for $^1O_2$ (E_T = 94 kJ/mol) in POA.

288 The COM photo-degradation can change the yield of $^1O_2$. Compared with original POA

289 samples, the signal intensity of $^1O_2$ decreases significantly in the samples with 7 days of photolysis

290 (the blue curve in **Fig.7A**), with an average decrease of 42.1% (**Fig.7C**), which prove that photo-

291 degradation has a attenuating effect on the photochemical activity. Similar to the original sample,

292 in the photolyzed samples, the signal intensity of $^1O_2$ does not decrease obviously when the high-

293 energy triplet states are quenched by sorbic acid. The mechanism is the same as the original samples.

294 The results also reveal that COM photo-degradation do not change the mechanism of low-energy

295 $^3COM^*$ inducing $^1O_2$ in POA.

296 The photochemical characteristics of ambient PM are different from POA. More narrowly,

297 there is no obvious $^1O_2$ signal in original ambient PM samples before light excitation (the red curve

298 in **Fig.7B (I)**). $^1O_2$ is also not generated after 60 min in dark (the red curve in **Fig.7B (II)**). The

299 content of $^1O_2$ increase significantly after 60 minutes of light excitation (the red curve in **Fig.7B**

300 **(III)**). When the triplet states are quenched by sorbic acid (**Fig.7B (IV)**), the signal of $^1O_2$ disappears.

301 The result suggests that $^1O_2$ is mainly induced by high-energy $^3COM^*$ in ambient PM. Compared

302 with the original samples, the signal intensity of $^1O_2$ decrease by 41.0% on average in photolyzed

303 samples (the red curve in **Fig.6B**). This characteristic suggests the attenuating effect of COM photo-

304 degradation on photochemical activity in ambient PM, which is similar to POA. However, the

305 quenching effect of sorbic acid on various aerosols are different (**Fig.7 (IV)**). The above results

306 directly show that the precursor of high-energy triplet states could be photolyzed, which directly

307 lead to the decrease of $^1O_2$ yield in the ambient PM. Other experiments are needed to study whether

308 the low-energy triplet precursors in POA are photolyzed and cause a decrease in the yield of $^1O_2$.

309
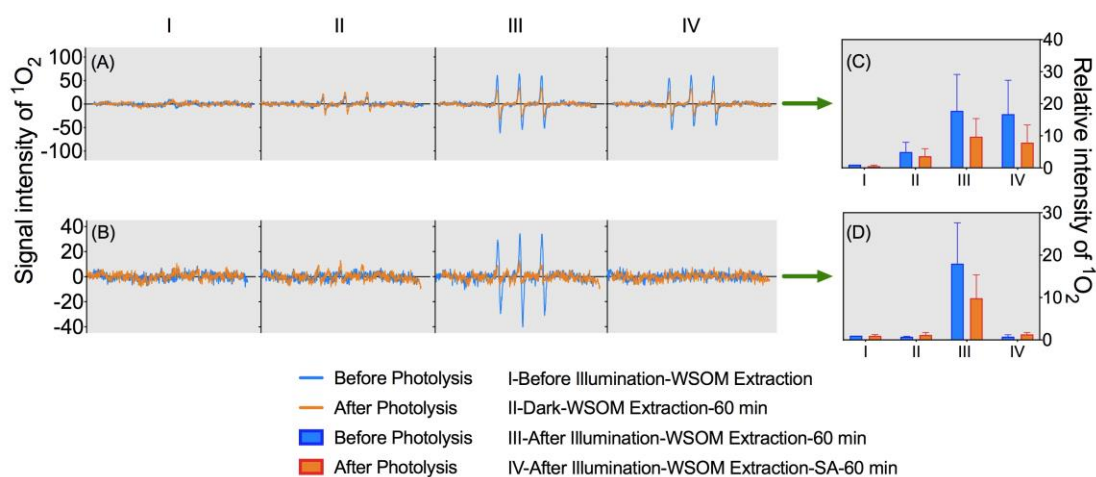
310 **Fig.7** Variations of DOM inducing $^1O_2$ before and after photolysis. (A) and (C) are the results obtained from POA

311 samples. (B) and (D) are the results obtained from Ambient PM. The left of the figure was the EPR spectra of $^1O_2$.

312 The right of the figure was the content variations of $^1O_2$. Relative content was calculated with a standard of the signal

313 intensity of $^1O_2$. The standard is the signal intensity of $^1O_2$, which is induced by un-photolyzed and un-illuminated

314 samples.

4. Implication

We made a comprehensive study of COM photo-degradation, changes in optical properties and chemical compositions, the effect of COM photo-degradation on photochemical activity and aerosol aging. The properties of COM photo-degradation were revealed. COM photo-degradation could be explained by reduction of carbonaceous components, decrease of light absorption capacity, and attenuation of fluorescence intensity. There are great differences in various COM in aerosols. Therefore, we suggested that the properties COM photo-degradation could be comprehensively characterized by carbonaceous components and optical characteristics. We studied that the photo-degradation could lead to COM decompose and change in types. High-molecular-weight DOM could be decomposed into low-molecular-weight DOM during photolysis. The conversion process of low-oxidation HULIS to high-oxidation HULIS is observed in ambient PM, which reflects the significant influence of photo-degradation on chemical composition. In turn, the attenuation and type conversion of COM provide an important basis to trace the aerosol aging process. Optical properties were also affected by COM photo-degradation.

The effects of COM photo-degradation on the photochemical activity in aerosols are studied. We evaluated the effect of COM photo-degradation on the photochemical activity. The ability of triplet state generation and $^1O_2$ yield was chosen to quantify the photochemical activity. Triplet state generation ability remain unchanged in ambient PM and increased in POA during aerosol aging. On the one hand, only a small amount of chromophore could generate $^3COM^*$ in aerosols. Thus, COM photo-degradation could not properly illustrate changes in $^3COM^*$. On the other hand, the energy of capturing agents was closely related to measured $^3COM^*$ and TMP may capture short-lived triplet state. Therefore, chromophores, that could form a short-lived triplet state, may not be reduced or even generated during photolysis. Photo-degradation has a significant attenuating effect on the $^1O_2$ yield. Therefore, photolysis and/or conversion of COM could be considered to be the main influence factor for photochemical reaction capacity. COM Photo-degradation indirectly affected the aerosols aging due to the changes in inducing reactive oxygen species. In addition, the photochemical reaction mechanisms and aerosol aging processes are relatively different in aerosols. It may be more useful to distinguish the types of $^3COM^*$ into high and low energies, so that the mechanism of COM photochemical reaction can be elucidated. In summary, the aerosol aging process has a remarkable impact on atmospheric photochemistry. Aerosol aging can not only change the type and content of COM, but also change their photochemical activity, which furtherly has a potential impact on the aerosol fate. Different types of aerosols have different aging mechanisms, so the environmental impacts caused by COM should also be different.

Data availability. All data that support the findings of this study are available in this article and its Supplement or from the corresponding author on request.

350 **Supporting information.** Additional details, including Tables S1−S5, Figures S1−S8, calculation

351 of optical characteristics of WSOM/WISOM, are contained in the SI.

352 **Author contributions.** QC and ZM designed the experiments and data analysis. ZM and LZ

353 performed sample collection. ZM performed the photochemical experiment. ZM and DG performed

354 the OC/EC analysis and optical analysis. HL performed the EPR analysis. QC prepared the paper

355 with the contributions from all co-authors.

356 **Competing interests.** The authors declare that they have no conflict of interest.

357 **Acknowledgments.** We thank the National Natural Resources Foundation for its financial support.

358 **Financial support.** This work was supported by the National Natural Science Foundation of China

359 (grant numbers 41877354 and 41703102).

References

361 Aiona, P. K., Luek, J. L., Timko, S. A., Powers, L. C., Gonsior, M., and Nizkorodov, S. A.: Effect of Photolysis on
362 Absorption and Fluorescence Spectra of Light-Absorbing Secondary Organic Aerosols, ACS Earth Space
363 Chem., 2, 235-245, 10.1021/acsearthspacechem.7b00153, 2018.
364 Alfarra, M. R., Prevot, A. S., Szidat, S., Sandradewi, J., Weimer, S., Lanz, V. A., Schreiber, D., Mohr, M., and
365 Baltensperger, U.: Identification of the mass spectral signature of organic aerosols from wood burning
366 emissions, Environ. Sci. Technol., 41, 5770-5777, http://dx.doi.org/10.1021/es062289b, 2007.
367 Altieri, K. E., Carlton, A. G., Lim, H. J., Turpin, B. J., and Seitzinger, S. P.: Evidence for oligomer formation in
368 clouds: Reactions of isoprene oxidation products, Environ. Sci. Technol., 40, 4956-4960,
369 http://dx.doi.org/10.1021/es052170n, 2006.
370 Altieri, K. E., Seitzinger, S. P., Carlton, A. G., Turpin, B. J., Klein, G. C., and Marshall, A. G.: Oligomers formed
371 through in-cloud methylglyoxal reactions: Chemical composition, properties, and mechanisms investigated by
372 ultra-high resolution FT-ICR mass spectrometry, Atmos. Environ., 42, 1476-1490,
373 http://dx.doi.org/10.1016/j.atmosenv.2007.11.015, 2008.
374 Andreae, M. O., and Gelencser, A.: Black carbon or brown carbon? The nature of light-absorbing carbonaceous
375 aerosols, Atmos. Chem. Phys., 6, 3131-3148, http://dx.doi.org/10.5194/acp-6-3131-2006, 2006.
376 Birdwell, J. E., and Engel, A. S.: Characterization of dissolved organic matter in cave and spring waters using
377 UV−Vis absorbance andfluorescence spectroscopy, Org. Geochem., 41,
378 http://dx.doi.org/10.1016/j.orggeochem.2009.11.002, 2010.
379 Chen, Q., Miyazaki, Y., Kawamura, K., Matsumoto, K., Coburn, S., Volkamer, R., Iwamoto, Y., Kagami, S., Deng,
380 Y., Ogawa, S., Ramasamy, S., Kato, S., Ida, A., Kajii, Y., and Mochida, M.: Characterization of Chromophoric
381 Water-Soluble Organic Matter in Urban, Forest, and Marine Aerosols by HR-ToF-AMS Analysis and
382 Excitation-Emission Matrix Spectroscopy, Environ. Sci. Technol., 50, 10351-10360,
383 http://dx.doi.org/10.1021/acs.est.6b01643, 2016a.
384 Chen, Q., Mu, Z., Xu, L., Wang, M., Wang, J., Shan, M., Yang, X., Fan, X., Song, J., Wang, Y., Lin, P., Zhang, L.,
385 Shen, Z., and Du, L.: Triplet State Formation of Chromophoric Dissolved Organic Matter in Atmospheric
386 Aerosols: Characteristics and Implications, Atmos. Chem. Phys. Discuss., https://doi.org/10.5194/acp-2019-
387 1032, 2020.
388 Chen, Q., Li, J., Hua, X., Jiang, X., Mu, Z., Wang, M., Wang, J., Shan, M., Yang, X., Fan, X., Song, J., Wang, Y.,
389 Guan, D., and Du, L.: Identification of species and sources of atmospheric chromophores by fluorescence
390 excitation-emission matrix with parallel factor analysis, Sci. Total Environ., 718, 137322,
391 http://dx.doi.org/10.1016/j.scitotenv.2020.137322, 2020.
392 Chen, Q. C., Ikemori, F., and Mochida, M.: Light Absorption and Excitation-Emission Fluorescence of Urban
393 Organic Aerosol Components and Their Relationship to Chemical Structure, Environ. Sci. Technol., 50, 10859-
394 10868, http://dx.doi.org/10.1021/acs.est.6b02541, 2016b.
395 Chen, Y., Zhang, X., and Feng, S.: Contribution of the Excited Triplet State of Humic Acid and Superoxide Radical
396 Anion to Generation and Elimination of Phenoxyl Radical, Environ. Sci. Technol., 52, 8283-8291,
397 http://dx.doi.org/10.1021/acs.est.8b00890, 2018.

Cheng, Y., He, K. B., Du, Z. Y., Engling, G., Liu, J. M., Ma, Y. L., Zheng, M., and Weber, R. J.: The characteristics of brown carbon aerosol during winter in Beijing, Atmos. Environ., 127, 355-364, http://dx.doi.org/10.1016/j.atmosenv.2015.12.035, 2016.

Chin, Y. P., Aiken, G., and O'Loughlin, E.: Molecular weight, polydispersity, and spectroscopic properties of aquatic humic substances, Environ. Sci. Technol., 28, 1853-1858, http://dx.doi.org/10.1021/es00060a015, 1994.

Chow, J. C., Watson, J. G., Chen, L. W., Arnott, W. P., Moosmuller, H., and Fung, K.: Equivalence of elemental carbon by thermal/optical reflectance and transmittance with different temperature protocols, Environ. Sci. Technol., 38, 4414-4422, http://dx.doi.org/10.1021/es034936u, 2004.

Chu, C. H., Lundeen, R. A., Sander, M., and McNeill, K.: Assessing the Indirect Photochemical Transformation of Dissolved Combined Amino Acids through the Use of Systematically Designed Histidine-Containing Oligopeptides, Environ. Sci. Technol., 49, 12798-12807, http://dx.doi.org/10.1021/acs.est.5b03498, 2015.

Coble, P. G.: Marine optical biogeochemistry: the chemistry of ocean color, Chem. Rev., 107, 402-418, http://dx.doi.org/10.1021/cr050350+, 2007.

Cory, R. M., and McKnight, D. M.: Fluorescence spectroscopy reveals ubiquitous presence of oxidized and reduced quinones in dissolved organic matter, Environ. Sci. Technol., 39, 8142-8149, http://dx.doi.org/10.1021/es0506962, 2005.

Del Vecchio, R., and Blough, N. V.: Photobleaching of chromophoricdissolved organic matter in natural waters: kinetics and modeling, Mar. Chem., 78, 231–253, http://dx.doi.org/10.1016/S0304-4203(02)00036-1, 2002.

Del Vecchio, R., and Blough, N. V.: On the origin of the optical properties of humic substances, Environ. Sci. Technol., 38, 3885-3891, http://dx.doi.org/10.1021/es049912h, 2004.

Duarte, R. M. B. O., Pio, C. A., and Duarte, A. C.: Spectroscopic study of the water-soluble organic matter isolated from atmospheric aerosols collected under different atmospheric conditions, Anal. Chim. Acta, 530, 7-14, http://dx.doi.org/10.1016/j.aca.2004.08.049, 2005.

Fellman, J. B., Miller, M. P., Cory, R. M., D'Amore, D. V., and White, D.: Characterizing Dissolved Organic Matter Using PARAFAC Modeling of Fluorescence Spectroscopy: A Comparison of Two Models, Environ. Sci. Technol., 43, 6228-6234, http://dx.doi.org/10.1021/es900143g, 2009.

Gonsior, M., Peake, B. M., Cooper, W. T., Podgorski, D., D'Andrilli, J., and Cooper, W. J.: Photochemically induced changes in dissolved organic matter identified by ultrahigh resolution fourier transform ion cyclotron resonance mass spectrometry, Environ. Sci. Technol., 43, 698-703, http://dx.doi.org/10.1021/es8022804, 2009.

Graber, E. R., and Rudich, Y.: Atmospheric HULIS: how humic-like are they? A comprehensive and critical review, Atmos. Chem. Phys., 6, 729-753, http://dx.doi.org/10.5194/acp-6-729-2006, 2005.

Grieshop, A. P., Donahue, N. M., and Robinson, A. L.: Laboratory investigation of photochemical oxidation of organic aerosol from wood fires 2: analysis of aerosol mass spectrometer data, Atmos. Chem. Phys., 9, 2227-2240, http://dx.doi.org/DOI 10.5194/acp-9-2227-2009, 2009.

Haag, W. R., and Gassman, E.: Singlet oxygen in surface waters-Part II: Quantum yields of its production by some natural humic materials as a function of wavelength, Chemosphere, 13, 641-650, http://dx.doi.org/10.1016/0045-6535(84)90200-5, 1984.

Harrison, A.W., Waterson, A.M., De Bruyn, W.J.: Spectroscopic and Photochemical Properties of Secondary Brown Carbon from Aqueous Reactions of Methylglyoxal, ACS Earth Space Chem., 4, 762-773, http://dx.doi.org/10.1021/acsearthspacechem.0c00061, 2020.

Haynes, J. P., Miller, K. E., and Majestic, B. J.: Investigation into Photoinduced Auto-Oxidation of Polycyclic Aromatic Hydrocarbons Resulting in Brown Carbon Production, Environ. Sci. Technol., 53, 682-691, http://dx.doi.org/10.1021/acs.est.8b05704, 2019.

Holmes, B. J., and Petrucci, G. A.: Water-soluble oligomer formation from acid-catalyzed reactions of levoglucosan in proxies of atmospheric aqueous aerosols, Environ. Sci. Technol., 40, 4983-4989, http://dx.doi.org/10.1021/es060646c, 2006.

Huguet, A., Vacher, L., Relexans, S., Saubusse, S., Froidefond, J. M., and Parlanti, E.: Properties of fluorescent dissolved organic matter inthe Gironde Estuary, Org. Geochem., 40, http://dx.doi.org/10.1016/j.orggeochem.2009.03.002, 2009.

Karanasiou, A., Minguillón, M. C., Viana, M., Alastuey, A., Putaud, J.-P., Maenhaut, W., Panteliadis, P., Močnik, G., Favez, O., and Kuhlbusch, T. A. J.: Thermal-optical analysis for the measurement of elemental carbon (EC) and organic carbon (OC) in ambient air a literature review, Atmos. Meas. Tech. Discuss., 8, 9649-9712, http://dx.doi.org/10.5194/amtd-8-9649-2015, 2015.

Kaur, R., and Anastasio, C.: First Measurements of Organic Triplet Excited States in Atmospheric Waters, Environ. Sci. Technol., 52, 5218-5226, http://dx.doi.org/10.1021/acs.est.7b06699, 2018.

Kieber, R. J., Adams, M. B., Wiley, J. D., Whitehead, R. F., Avery, G. B., Mullaugh, K. M., and Mead, R. N.: Short term temporal variability in the photochemically mediated alteration of chromophoric dissolved organic matter (CDOM) in rainwater, Atmos. Environ., 50, 112-119, http://dx.doi.org/10.1016/j.atmosenv.2011.12.054, 2012.

Korak, J. A., Dotson, A. D., Summers, R. S., and Rosario-Ortiz, F. L.: Critical analysis of commonly used fluorescence metrics to characterize dissolved organic matter, Water Res., 49, 327-338, http://dx.doi.org/10.1016/j.watres.2013.11.025, 2014.

Latch, D. E., and McNeill, K.: Microheterogeneity of singlet oxygen distributions in irradiated humic acid solutions, Science, 311, 1743-1747, http://dx.doi.org/10.1126/science.1121636, 2006.

Lee, H. J., Laskin, A., Laskin, J., and Nizkorodov, S. A.: Excitation-emission spectra and fluorescence quantum yields for fresh and aged biogenic secondary organic aerosols, Environ. Sci. Technol., 47, 5763-5770, http://dx.doi.org/10.1021/es400644c, 2013.

Lee, H. J., Aiona, P. K., Laskin, A., Laskin, J., and Nizkorodov, S. A.: Effect of solar radiation on the optical properties and molecular composition of laboratory proxies of atmospheric brown carbon, Environ. Sci. Technol., 48, 10217-10226, http://dx.doi.org/10.1021/es502515r, 2014.

Liu, J. M., Lin, P., Laskin, A., Laskin, J., Kathmann, S. M., Wise, M., Caylor, R., Imholt, F., Selimovic, V., and Shilling, J. E.: Optical properties and aging of light-absorbing secondary organic aerosol, Atmos. Chem. Phys., 16, 12815-12827, http://dx.doi.org/10.5194/acp-16-12815-2016, 2016.

Ma, J., Del Vecchio, R., Golanoski, K. S., Boyle, E. S., and Blough, N. V.: Optical properties of humic substances and CDOM: effects of borohydride reduction, Environ. Sci. Technol., 44, 5395-5402, http://dx.doi.org/10.1021/es100880q, 2010.

Maizel, A. C., Li, J., and Remucal, C. K.: Relationships Between Dissolved Organic Matter Composition and Photochemistry in Lakes of Diverse Trophic Status, Environ. Sci. Technol., 51, 9624-9632, http://dx.doi.org/10.1021/acs.est.7b01270, 2017.

Malley, P. P. A., Grossman, J. N., and Kahan, T. F.: Effects of Chromophoric Dissolved Organic Matter on Anthracene Photolysis Kinetics in Aqueous Solution and Ice, J. Phys. Chem. A, 121, 7619-7626, http://dx.doi.org/10.1021/acs.jpca.7b05199, 2017.

McKnight, D. M., Boyer, E. W., Westerhoff, P. K., Doran, P. T., Kulbe, T., and Andersen, D. T.: Spectrofluorometric characterization of dissolved organic matter for indication of precursor organic material and aromaticity, Limnol. Oceanogr., 46, 38-48, http://dx.doi.org/10.4319/lo.2001.46.1.0038, 2001.

McNeill, K., and Canonica, S.: Triplet state dissolved organic matter in aquatic photochemistry: reaction mechanisms, substrate scope, and photophysical properties, Environ. Sci. Process Impacts, 18, 1381-1399, http://dx.doi.org/10.1039/c6em00408c, 2016.

Moor, K. J., Schmitt, M., Erickson, P. R., and McNeill, K.: Sorbic Acid as a Triplet Probe: Triplet Energy and Reactivity with Triplet-State Dissolved Organic Matter via 1O2 Phosphorescence, Environ. Sci. Technol., http://dx.doi.org/10.1021/acs.est.9b01787, 2019.

Mu, Z., Chen, Q. C., Wang, Y. Q., Shen, Z. X., Hua, X. Y., Zhang, Z. M., Sun, H. Y., Wang, M. M., and Zhang, L. X.: Characteristics of Carbonaceous Aerosol Pollution in PM2.5 in Xi'an, Huan Jing Ke Xue, 40, 1529-1536, http://dx.doi.org/10.13227/j.hjkx.201807135, 2019.

Murphy, K. R., Stedmon, C. A., Waite, T. D., and Ruiz, G. M.: Distinguishing between terrestrial and autochthonous organic matter sources in marine environments using fluorescence spectroscopy, Mar. Chem., 108, 40-58, http://dx.doi.org/10.1016/j.marchem.2007.10.003, 2008.

Murphy, K. R., Stedmon, C. A., Graeber, D., and Bro, R.: Fluorescence spectroscopy and multi-way techniques. PARAFAC, Anal. Methods, 5, 6557-6566, http://dx.doi.org/10.1039/c3ay41160e, 2013.

Murphy, K.R., Timko, S.A., Gonsior, M., Powers, L.C., Wünsch, U.J., Stedmon, C.A.: Photochemistry Illuminates Ubiquitous Organic Matter Fluorescence Spectra, Environ. Sci. Tech., 52, 11243-11250, http://dx.doi.org/ 10.1021/acs.est.8b02648, 2018.

Paul Hansard, S., Vermilyea, A. W., and Voelker, B. M.: Measurements of superoxide radical concentration and decay kinetics in the Gulf of Alaska, Deep Sea Res., Part I, 57, 1111-1119, http://dx.doi.org/10.1016/j.dsr.2010.05.007, 2010.

Perri, M. J., Seitzinger, S., and Turpin, B. J.: Secondary organic aerosol production from aqueous photooxidation of glycolaldehyde: Laboratory experiments, Atmos. Environ., 43, 1487-1497, http://dx.doi.org/10.1016/j.atmosenv.2008.11.037, 2009.

Powers, L. C., Babcock-Adams, L. C., Enright, J. K., and Miller, W. L.: Probing the photochemical reactivity of deep ocean refractory carbon (DORC): Lessons from hydrogen peroxide and superoxide kinetics, Mar. Chem., 177, 306-317, 10.1016/j.marchem.2015.06.005, 2015.

Richards-Henderson, N. K., Pham, A. T., Kirk, B. B., and Anastasio, C.: Secondary organic aerosol from aqueous reactions of green leaf volatiles with organic triplet excited states and singlet molecular oxygen, Environ. Sci. Technol., 49, 268-276, http://dx.doi.org/10.1021/es503656m, 2015.

Rosado-Lausell, S.L., Wang, H.T., Gutierrez, L., Romero-Maraccini, O.C., Niu, X.Z., Gin, K.Y.H., Croue, J.P., Nguyen, T.H.: Roles of singlet oxygen and triplet excited state of dissolved organic matter formed by different organic in bacteriophage MS2 inactivation, Water Res., 47, 4869-4879, http://dx.doi.org/10.1016/j.watres.2013.05.018, 2013.

Rosario-Ortiz, F. L., and Canonica, S.: Probe Compounds to Assess the Photochemical Activity of Dissolved Organic Matter, Environ. Sci. Technol., 50, 12532-12547, http://dx.doi.org/10.1021/acs.est.6b02776, 2016.

Saleh, R., Hennigan, C. J., McMeeking, G. R., Chuang, W. K., Robinson, E. S., Coe, H., Donahue, N. M., and Robinson, A. L.: Absorptivity of brown carbon in fresh and photo-chemically aged biomass-burning emissions, Atmos. Chem. Phys., 13, 7683-7693, http://dx.doi.org/10.5194/acp-13-7683-2013, 2013.

Sharpless, C. M.: Lifetimes of Triplet Dissolved Natural Organic Matter (DOM) and the Effect of NaBH4 Reduction on Singlet Oxygen Quantum Yields: Implications for DOM Photophysics, Environ. Sci. Technol., 46, 4466-4473, http://dx.doi.org/10.1021/es300217h, 2012.

Sierra, M. M. D., Giovanela, M., Parlanti, E., and Soriano-Sierra, E. J.: Fluorescence fingerprint of fulvic and humic acids from varied originsas viewed by single-scan and excitation/emission matrix techniques, Chemosphere, 58, http://dx.doi.org/10.1016/j.chemosphere.2004.09.038, 2005.

Smith, J. D., Sio, V., Yu, L., Zhang, Q., and Anastasio, C.: Secondary organic aerosol production from aqueous reactions of atmospheric phenols with an organic triplet excited state, Environ. Sci. Technol., 48, 1049-1057, http://dx.doi.org/10.1021/es4045715, 2014.

Szymczak, R., and Waite, T.: Generation and decay of hydrogen peroxide in estuarine waters, Mar. Freshwater Res., 39, 289-299, http://dx.doi.org/10.1071/MF9880289, 1988.

531 Tang, J., Li, J., Su, T., Han, Y., Mo, Y.Z., Jiang, H.X., Cui, M., Jiang, B., Chen, Y.J., Tang, J.H., Song, J.Z., Peng,
532   P.A., Zhang, G.: Molecular compositions and optical properties of dissolved brown carbon in biomass burning,
533   coal combustion, and vehicle emission aerosols illuminated by excitation-emission matrix spectroscopy and
534   Fourier transform ion cyclotron resonance mass spectrometry analysis. Atmos. Chem. Phys. 20, 2513-2532,
535   http://dx.doi.org/10.5194/acp-20-2513-2020, 2020.
536 Tang, S. S., Li, F. H., Tsona, N. T., Lu, C. Y., Wang, X. F., and Du, L.: Aqueous-Phase Photooxidation of Vanillic
537   Acid: A Potential Source of Humic-Like Substances (HULIS), Acs Earth and Space Chem., 4, 862-872,
538   http://dx.doi.org/10.1021/acsearthspacechem.0c00070, 2020.
539 Vodacek, A., Blough, N. V., DeGrandpre, M. D., Peltzer, E. T., and Nelson, R. K.: Seasonal Variation of
540   CDOM and DOC in theMiddle Atlantic Bight: Terrestrial Inputs and Photooxidation, Limnol.
541   Oceanogr., 42, 231-253, http://dx.doi.org/10.1117/12.26643, 1997.
542 Wenk, J., von Gunten, U., and Canonica, S.: Effect of dissolved organic matter on the transformation of contaminants
543   induced by excited triplet states and the hydroxyl radical, Environ. Sci. Technol., 45, 1334-1340,
544   http://dx.doi.org/10.1021/es102212t, 2011.
545 Wenk, J., Aeschbacher, M., Salhi, E., Canonica, S., von Gunten, U., and Sander, M.: Chemical oxidation of dissolved
546   organic matter by chlorine dioxide, chlorine, and ozone: effects on its optical and antioxidant properties,
547   Environ. Sci. Technol., 47, 11147-11156, http://dx.doi.org/10.1021/es402516b, 2013.
548 Wong, J. P. S., Zhou, S. M., and Abbatt, J. P. D.: Changes in Secondary Organic Aerosol Composition and Mass
549   due to Photolysis: Relative Humidity Dependence, J. Phys. Chem. A, 119, 4309-4316,
550   http://dx.doi.org/10.1021/jp506898c, 2015.
551 Zappoli, S., Andracchio, A., Fuzzi, S., Facchini, M. C., Gelencser, A., Kiss, G., Krivacsy, Z., Molnar, A., Meszaros,
552   E., Hansson, H. C., Rosman, K., and Zebuhr, Y.: Inorganic, organic and macromolecular components of fine
553   aerosol in different areas of Europe in relation to their water solubility, Atmos. Environ., 33, 2733-2743,
554   http://dx.doi.org/10.1016/S1352-2310(98)00362-8, 1999.
555 Zepp, R. G., Schlotzhauer, P. F., and Sink, R. M.: Photosensitized transformations involving electronic energy
556   transfer in natural waters: role of humic substances, Environ. Sci. Technol., 19, 74-81,
557   http://dx.doi.org/10.1021/es00131a008, 1985.
558 Zhang, D., Yan, S., and Song, W.: Photochemically induced formation of reactive oxygen species (ROS) from
559   effluent organic matter, Environ. Sci. Technol., 48, 12645-12653, http://dx.doi.org/10.1021/es5028663, 2014.
560 Zhao, R., Lee, A. K. Y., Huang, L., Li, X., Yang, F., and Abbatt, J. P. D.: Photochemical processing of aqueous
561   atmospheric brown carbon, Atmos. Chem. Phys., 15, 6087-6100, http://dx.doi.org/10.5194/acp-15-6087-2015,
562   2015.
563 Zhong, M., and Jang, M.: Dynamic light absorption of biomass-burning organic carbon photochemically aged under
564   natural sunlight, Atmos. Chem. Phys., 14, 1517-1525, http://dx.doi.org/10.5194/acp-14-1517-2014, 2014.
565 Zhou, H., Yan, S., Lian, L., and Song, W.: Triplet-State Photochemistry of Dissolved Organic Matter: Triplet-State
566   Energy Distribution and Surface Electric Charge Conditions, Environ. Sci. Technol., 53, 2482-2490,
567   http://dx.doi.org/10.1021/acs.est.8b06574, 2019.